

Metallic phase between the Fermi glass and the Wigner crystal in two dimensions

X. Waintal¹, G. Benenti¹, and J.-L. Pichard¹

¹CEA, Service de Physique de l'Etat Condensé,
Centre d'Etudes de Saclay, F-91191 Gif-sur-Yvette, France
pichard@spec.saclay.cea.fr

Received 21 July 1999, accepted dd.mm.yyyy by ue

Abstract. For intermediate Coulomb energy to Fermi energy ratios r_s , spinless fermions in a two-dimensional random potential form a new quantum phase, different from the Fermi glass (weakly interacting Anderson localized states) and the Wigner crystal (regular array of charges pinned by the disorder). The intermediate phase is characterized by an ordered flow of persistent currents with a typical value decreasing with excitation energy. Extending finite size scaling analysis to the many body ground state, we find that electron-electron interactions can drive the Fermi glass towards an intermediate metallic phase (Coulomb metal).

Keywords: $2d$ metal-insulator transition, Anderson localization, interacting fermions

PACS: 71.30.+h, 72.15.Rn, 71.27.+a

1 Introduction

According to the scaling theory of localization [1], all states are localized for non-interacting particles in two dimensions ($2d$). This absence of a metallic state in $2d$ is nowadays challenged since a lot of transport measurements, following the pioneering experiments of Kravchenko and co-workers [2], give evidence of an insulator-metal transition (IMT) when the carrier density is increased. Many experimental results suggest that Coulomb repulsion drives this phenomenon: (1) In a very clean heterostructure the IMT was observed at a Coulomb energy to Fermi energy ratio $r_s \approx 35$ [3], close to $r_s \approx 37$ for which a clean Wigner crystal melts according to Monte Carlo simulations [4]; (2) In more disordered samples, the IMT typically occurs at $r_s \approx 10$, again compatible with the value expected for the melting of a pinned Wigner crystal [5]; (3) At a weaker r_s interactions no longer dominate and a re-entry towards an insulating phase (Fermi glass of weakly interacting localized particles) was observed at $r_s \approx 6$ in [6]. As at the IMT $k_F l \approx 1$ (k_F denoting the Fermi wave vector and l the elastic mean free path), disorder is important and has to be considered, together with interactions, in a non perturbative way.

Taking advantage of numerical techniques, we consider a model of N Coulomb interacting spinless fermions in a disordered square lattice with L^2 sites. The Hamiltonian reads:

$$H = -t \sum_{\langle i,j \rangle} c_i^\dagger c_j + \sum_i v_i n_i + U \sum_{i \neq j} \frac{n_i n_j}{2r_{ij}}, \quad (1)$$

where c_i^\dagger (c_i) creates (destroys) an electron in the site i , t is the strength of the hopping terms between nearest neighbours ($t = 1$ in the following) and r_{ij} the interparticle distance for a $2d$ torus. The random potential v_i of the site $i = (i_x, i_y)$ with occupation number $n_i = c_i^\dagger c_i$ is taken from a box distribution of width W . The interaction strength U yields $r_s = U/(2t\sqrt{\pi n_e})$ for a filling factor $n_e = N/L^2$. A Fermi golden rule approximation for the elastic scattering time leads, for $n_e \ll 1$, to $k_F l \approx 192\pi n_e (t/W)^2$.

2 Persistent currents

To measure delocalization effects induced by interactions, we study the sensitivity of the ground state to a change in the boundary conditions [7]. Boundary conditions are always taken periodic in the transverse y -direction, and such that the system encloses an Aharonov-Bohm flux ϕ in the longitudinal x -direction. Imposing $\phi = \pi/2$ ($\phi = \pi$ corresponds to anti-periodic boundary conditions), one drives a persistent current of total longitudinal and transverse components given by

$$I_l = -\frac{\partial E_0}{\partial \phi} = \frac{\sum_i I_i^l}{L} \quad \text{and} \quad I_t = \frac{\sum_i I_i^t}{L}, \quad (2)$$

with E_0 ground state energy. The local current I_i^l flowing at the site i in the longitudinal direction is defined by $I_i^l = 2\text{Im}\langle \Psi_0 | c_{i_x+1, i_y}^\dagger c_{i_x, i_y} | \Psi_0 \rangle$, with an analogous expression for I_i^t ($|\Psi_0\rangle$ is the ground state wavefunction). The response is paramagnetic if $I_l > 0$ and diamagnetic if $I_l < 0$. Exact diagonalization techniques (Lanczos method) are possible only for small system sizes and here we consider $N = 4$ particles in $L^2 = 36$ sites, for $W = 5, 10, 15$ ($k_F l = 2.7, 0.7, 0.3$ respectively) and $0 \leq r_s \leq 42$. We summarize in Fig. 1 results from a statistical study of an ensemble of 10^3 clusters. $|I_l|$ and $|I_t|$ have acceptable log-normal distributions for all values of r_s when $W \geq 5$ [7] and therefore the log-averages shown in Fig. 1 can be considered as typical values of the persistent currents: $I_{l,\text{typ}} = \exp \langle \ln |I_l| \rangle$, with an analogous expression for $I_{t,\text{typ}}$ (brackets indicate ensemble average). Fig. 1 (a) shows that the ground state transverse current is suppressed before the longitudinal current. It is then possible to single out an intermediate phase, in which the local currents flow in an ordered way along the direction imposed by the flux [7, 8]. This behaviour is evident in Fig. 1 (b): the ground state local current angles $\theta_i = \arctan(I_i^t/I_i^l)$ undergo a transition from a nearly uniform angular distribution (glass of currents randomly directed in the plane) towards a distribution strongly peaked in the longitudinal direction. As a consequence, the sign of the magnetic response becomes independent of the microscopic realization of the random potential (see Fig. 1 (b) insert). Notice that, for a not too strong disorder ($k_F l > 1$), in the intermediate phase $I_{l,\text{typ}}$ is enhanced by interactions up to a factor 3 (for $W = 5$, $r_s \approx 6$) before being suppressed due to charge crystallization [7]. Fig. 1 (c) displays the behaviour of the longitudinal current for the 20 lowest energy levels. The enhancement in $I_{l,\text{typ}}$ disappears away from the ground state. In addition, it is possible to identify three different regimes when $W = 5$: for approximately $r_s < 2$ and $r_s > 17$ the longitudinal current increases with the excitation energy ϵ , all

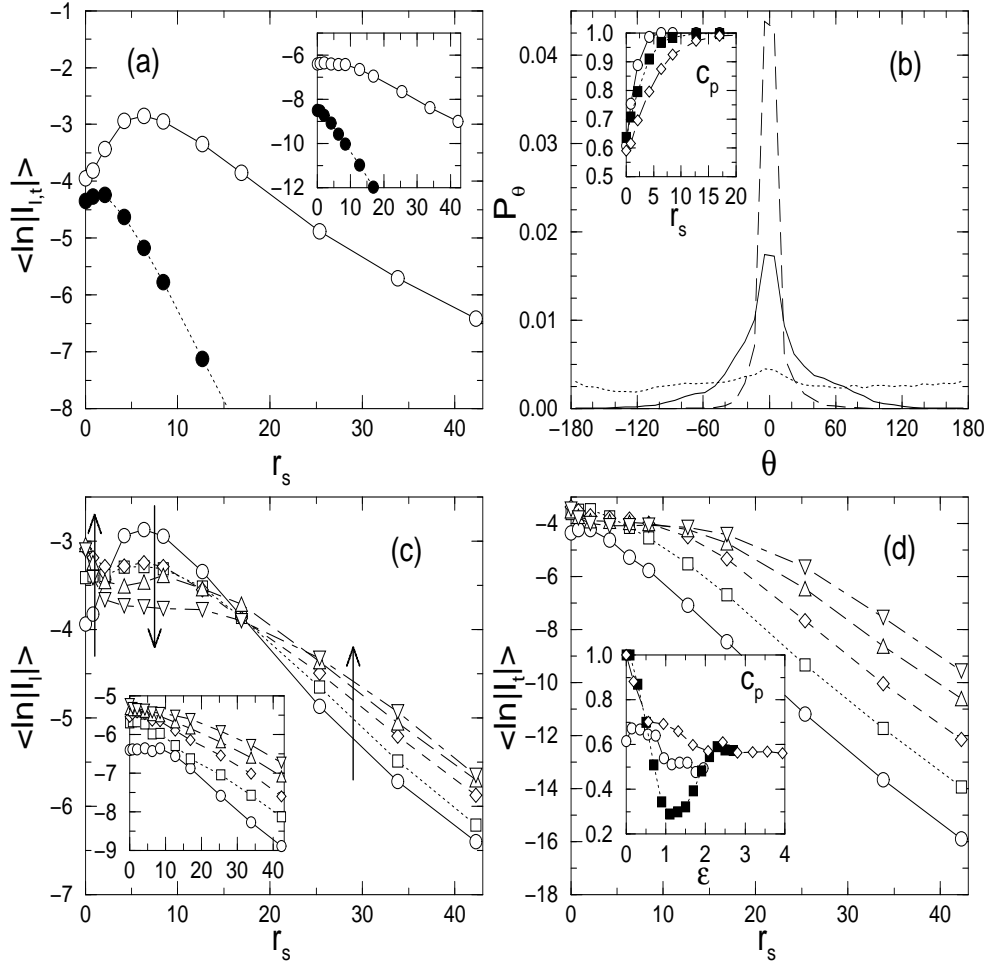


Fig. 1 (a) Log-averages of the ground state longitudinal current I_l (open circles) and transverse current I_t (filled circles) at $W = 5$. Inset: the same at $W = 15$. (b) Distribution P_θ of the ground state local currents angles at $W = 5$, for $r_s = 0$ (dotted line), $r_s = 6.3$ (full line), and $r_s = 42$ (dashed line). Inset: fraction c_p of paramagnetic samples for $W = 5$ (circles), $W = 10$ (squares) and $W = 15$ (diamonds). (c) Log-average of the longitudinal current at $W = 5$, for the ground state (circles), the first excited state (squares), the second-fourth excited states (diamonds), the fifth-ninth excited states (triangles up), and the tenth-nineteenth excited states (triangles down). Arrows indicate increase (or decrease) of the longitudinal current with excitation energy. Inset: the same at $W = 15$. (d) Same as in (c) but for the transverse current at $W = 5$. Inset: fraction of paramagnetic samples as a function of the excitation energy ϵ at $W = 5$, for $r_s = 0$ (circles), $r_s = 6.3$ (squares), and $r_s = 42$ (diamonds).

the contrary for intermediate r_s values. We remind that experimentally the metallic (insulating) phase has been identified [2, 3, 6] from a decrease (increase) with temperature of a related transport property, the conductance. For $W = 15$, $I_{l,\text{typ}}$ always decreases with ϵ (Fig. 1 (c) insert), indicating that a too strong disorder probably forbids a metallic phase in the thermodynamic limit. Fig. 1 (d) shows that, increasing ϵ , the transverse current is suppressed at larger r_s values, eventually compatible with r_s values at which the longitudinal current is suppressed. This fact suggests that the intermediate phase is destroyed at large enough temperatures. For $\epsilon > 2$ (the Fermi energy is given by $\epsilon_F = \pi n_e t = 0.35$) the sign of the persistent current is disorder dependent at any r_s value (Fig. 1 (d) insert).

3 Finite size scaling for the N body localization length

Though small clusters exhibit an enhancement of I_l for intermediate r_s , exact diagonalization does not allow to vary system size and to establish if the intermediate phase is metallic at the thermodynamic limit. In order to answer this question and to understand how Coulomb interaction destroys Anderson localization, we extend [9] finite size scaling analysis [10, 11] to interacting systems. We consider an ensemble of 5×10^3 clusters with $N = 3, 4, 5$ particles in square lattices of size $L = 24, 28, 31$ respectively, corresponding to very low filling factors $n_e \approx 5 \times 10^{-3}$. To have Anderson localization inside these sizes we consider a large disorder to hopping ratio $W/t = 10$. Therefore the low energy tail of the one body (1B) spectrum is made of impurity states trapped at some site i of exceptionally low v_i . As we are interested in studying the effect of Coulomb repulsion on genuine Anderson localized states we get rid of the band tail. Typically we ignore the $L^2/2$ first 1B levels (but results do not change provided that the Fermi level is out of the band tail, $\epsilon_F > -4t$; under this condition one can roughly estimate $k_{Fl} \approx 1$). From this restricted subset of 1B states we build a basis for the N body (NB) problem, truncated to the $N_H = 10^3$ Slater determinants of lowest energy (convergence tests are discussed in [9]). The scaling ansatz for the NB problem reads

$$\frac{\xi_L}{L} = f\left(\frac{L}{\xi}\right), \quad (3)$$

where we assume it is possible to map the localization length ξ_L at the system size L onto a scaling curve $f(L/\xi)$, with ξ characteristic scaling length of the infinite system. To characterize the NB ground state by a suitable localization length ξ_L , we consider the change $\delta\rho_j$ of the charge density induced by a small change δv_i of the random potential v_i located at a distance $|i - j|$. To improve the statistical convergence, we calculate more precisely the change $\delta\rho(r) = \sum_{j_y} \delta\rho_{r,j_y}$ of the charge density on the L sites of coordinate $j_x = r$ yielded by the change $v_{0,i_y} \rightarrow 1.01v_{0,i_y}$ for the L random potentials of coordinate $i_x = 0$. Fig. 2 (a) shows that $|\delta\rho(r)|$ is reasonably fitted by a log-normal distribution. Therefore it makes sense to characterize the typical strength of the fluctuations by $\delta\rho_{\text{typ}}(r) = \exp \langle \ln |\delta\rho(r)| \rangle$ and extract the length ξ_L over which the perturbation is effective from the exponential decay $\delta\rho_{\text{typ}}(r) \propto \exp(-r/\xi_L)$. Such a decay occurs only over a scale $r \ll L/2$ since the boundary conditions are periodic. In Fig. 2 (b) the lengths ξ_L are obtained from the slope of the linear parts

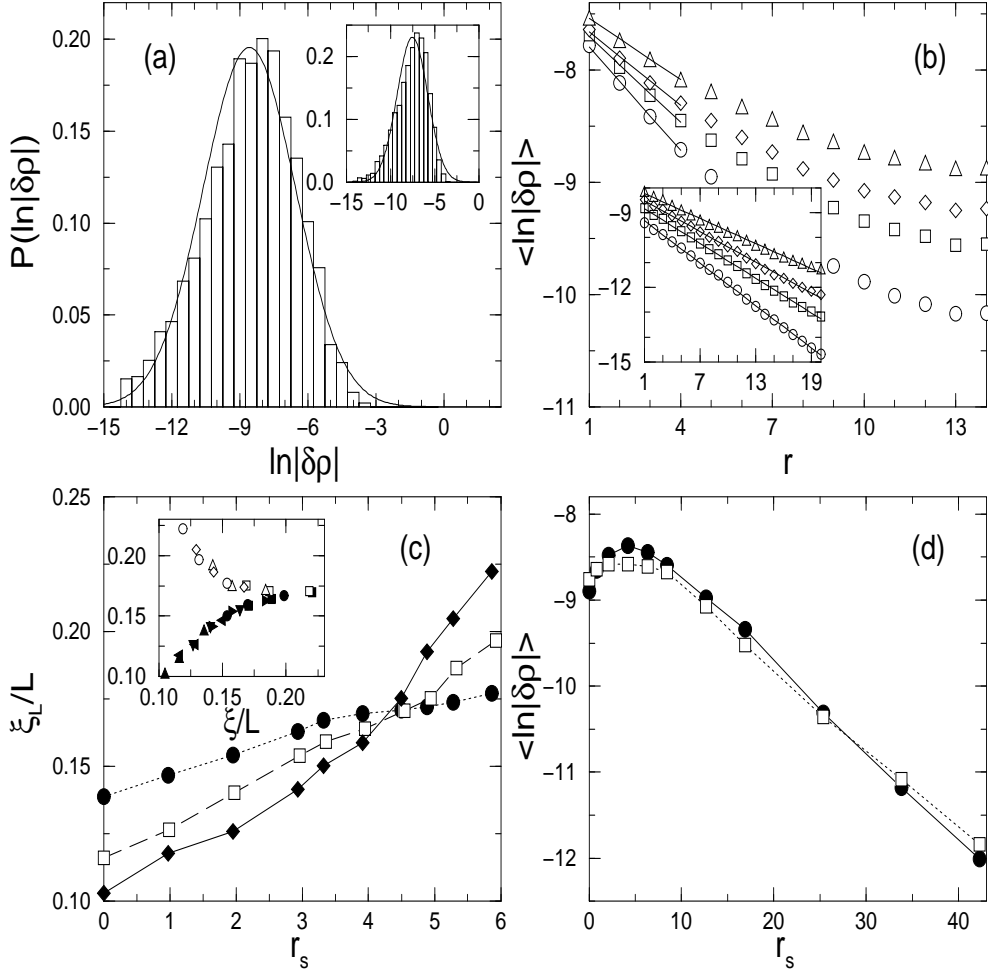


Fig. 2 (a) Distribution of the logarithms of the charge density variation $|\delta\rho|$ for $L = 31$, $r_s = 0$, $W = 10$, $r = 5$, fitted by a log-normal function of mean $\mu = -8.6$ and variance $\sigma^2 = 4.2$. Inset: the same at $r_s = 5.9$, with $\mu = -7.5$, $\sigma^2 = 3.0$. (b) Log-average of $|\delta\rho|$ as a function of r , for $L = 28$, $W = 10$, $r_s = 0$ (circles), $r_s = 2.0$ (squares), $r_s = 3.9$ (diamonds), and $r_s = 5.9$ (triangles). The lengths ξ_L are given by the inverse slopes of the straight lines. Inset: the same for a quasi-one dimensional geometry ($L_x = 80$, $L_y = 8$) at $W = 8$ (ensemble of 10^3 clusters). (c) Reduced localization length ξ_L/L as a function of r_s for $W = 10$, $L = 24$ (circles), $L = 28$ (squares), $L = 31$ (diamonds). Inset: ratios ξ_L/L mapped onto the scaling curve f as a function of the reduced scaling length ξ/L . Localized branch (filled symbols): $r_s = 0$ (triangles up), $r_s = 1.0$ (triangles left), $r_s = 2.0$ (triangles down), $r_s = 2.9$ (triangles right), $r_s = 3.3$ (circles), $r_s = 3.9$ (squares). Delocalized branch (open symbols): $r_s = 4.5$ (squares), $r_s = 4.9$ (triangles), $r_s = 5.3$ (diamonds), $r_s = 5.9$ (circles). (d) Log-average of $|\delta\rho|$ as a function of r_s for $N = 4$ particles in a 6×6 lattice, $r = 1$, $W = 5$ (circles) and $W = 15$ (squares) (ensemble of 5×10^2 clusters). 1B states are filled in starting from the lowest energy one.

of the curves (straight lines). A good exponential decay on a much larger interval can be observed in a quasi one dimensional geometry ($L_x \gg L_y$). Fig. 2 (c) gives how the reduced localization length ξ_L/L depends on r_s for the three considered sizes. A critical point appears at $r_s^F \approx 4.3$: for $r_s < r_s^F$, ξ_L/L decreases with L (Fermi glass) while it increases for $r_s > r_s^F$ (Coulomb metal). Fig. 2 (c) insert verifies the scaling ansatz (3): assuming suitable scaling lengths ξ all the data can be mapped onto a single scaling curve f , which develops two branches, as typical of second order phase transitions (like the 1B Anderson transition in three dimensions [10, 11]). A power fit of $\xi \propto |r_s - r_s^F|^{-\nu}$ yields a rough estimate for the critical exponent $\nu \approx 4$. In the quasi one dimensional case we were able to detect a strong interaction induced enhancement of the localization length (see Fig. 2 (b) insert) but no signature of a phase transition. Fig. 2 (d) shows that a local perturbation in the random potential plays a role similar to a change in the boundary conditions. For the small system sizes accessible to exact diagonalization it is not possible to extract the length ξ_L . However, it is possible to see how the typical value $\delta\rho_{\text{typ}}(r)$, evaluated for example when $r = 1$, evolves with r_s . This quantity increases in the intermediate phase before decreasing due to charge crystallization. Unfortunately it is not possible, within the approximate technique described above, to evaluate how ξ_L changes with L in the Wigner crystal phase.

4 Conclusions

Coulomb repulsion can drive a two dimensional system of spinless fermions in a random potential towards a new metallic phase, the Coulomb metal, which is different from the Fermi glass and the Wigner crystal. The local current I_i could be the order parameter driving the Fermi glass-Coulomb metal transition (through θ_i) and the Coulomb metal-Wigner crystal transition (through $|I_i|$).

This work is partially supported by the TMR network ‘‘Phase coherent dynamics of hybrid nanostructures’’ of the EU.

References

- [1] E. Abrahams, P. W. Anderson, D. C. Licciardello, and T. V. Ramakrishnan, Phys. Rev. Lett. **42** (1979) 673
- [2] S. V. Kravchenko, G. V. Kravchenko, J. E. Furneaux, V. M. Pudalov, and M. D’Iorio, Phys. Rev. B **50** (1994) 8039
- [3] J. Yoon, C. C. Li, D. Shahar, D. C. Tsui, and M. Shayegan, Phys. Rev. Lett. **82** (1999) 1744
- [4] B. Tanatar and D. M. Ceperley, Phys. Rev. B **39** (1989) 5005
- [5] S. T. Chui and B. Tanatar, Phys. Rev. Lett. **74** (1995) 458
- [6] A. R. Hamilton, M. Y. Simmons, M. Pepper, E. H. Linfield, P. D. Rose, and D. A. Ritchie, Phys. Rev. Lett. **82** (1999) 1542
- [7] G. Benenti, X. Waintal, and J.-L. Pichard, cond-mat/9904096, accepted for publication in Phys. Rev. Lett.
- [8] R. Berkovits and Y. Avishai, Phys. Rev. B **57** (1998) R15076
- [9] X. Waintal, G. Benenti, and J.-L. Pichard, cond-mat/9906397
- [10] J.-L. Pichard and G. Sarma, J. Phys. C: Solid State Phys. **14** (1981) L127
- [11] A. MacKinnon and B. Kramer, Phys. Rev. Lett. **47** (1981) 1546